Linear High-Force "Step And Repeat" Piezoelectric Motors

J.S.N. Paine*, M.E. Johns*, J.J. Sesler*, M.T. Stefanick* and J.A. Kennedy*

Abstract

Dynamic Structures and Materials, LLC (DSM) has designed a patent-pending piezoelectric linear motor for demonstration in two aerospace applications related to the operation of a cryogenic 2" isolation valve and an environmental controls air handling system for next-generation space vehicles. The scaleable actuator technology provides a combination of force, stroke, and speed not previously demonstrated in other piezoelectric motor developments. The IMPULSE PiezoMotor™ technology is presented as a viable and superior replacement for heritage pneumatic, hydraulic, and electromagnetic actuation devices. A key feature of the IMPULSE PiezoMotor™ technology resulting from its friction-based drive architecture is a power-off-lock characteristic (fails in last position). A description of the mechanism and key performance parameters (step size, drive force, and resolution/accuracy), influence of materials on friction/wear, and power requirements are discussed.

Introduction to Piezoelectric Motors

A development effort to produce linear proportional electromechanical actuators for valve control has resulted in a new class of linear actuation mechanisms based on piezoelectric prime movers. The piezoelectric driven actuators are based on a step and repeat motor topology that enables relatively large strokes compared to typical piezoelectric driven actuators. This paper describes the mechanism and how it operates as well as discusses design and performance issues relative to using this device in precision motion control applications.

Linear "Step and Repeat" piezoelectric motors or SRMs are electro-mechanical energy transducers that convert electrical energy to mechanical motion through the expansion of piezoelectric ceramic materials. Piezoelectricity is the ability of certain crystals to generate a voltage in response to applied mechanical stress. The piezoelectric effect is reversible in that piezoelectric crystals formed into thin layers and stacked with electrodes can expand a small amount when subjected to an externally applied voltage. Typical expansion of these "stacks" can be on the order of 0.1 to 0.2% of length (i.e. a 20 mm long sample will extend ~ 20 to 40 microns (0.001 to 0.0016") at an applied voltage of 100 to 200 VDC. Figure 1 illustrates the expansion for a simple prismatic piezoelectric ceramic stack actuator. The expansion can occur at very fast response times (20+ kHz) and relative high force (50 MPa). This high force can be harnessed to produce very high bandwidth actuators and motors.

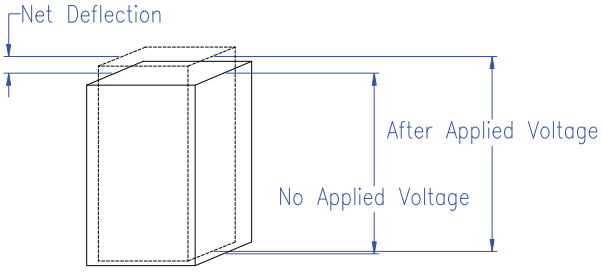

Figure 1 – Exaggerated Expansion Of A Piezoelectric Stack In The Column Direction

* Dynamic Structures and Materials, LLC, Franklin, TN

Piezoelectric stacks are the core components of DSM's SRM actuators. Since the single move displacement of piezoelectric ceramic stacks is very small, SRMs consist of a mechanism to convert many small steps into a single continuous move equaling the sum of the small steps. Generally, controlled intermittent friction is used as the means of transferring the displacement of the piezoelectric ceramic stack to the output shaft or slider's continuous motion. Spanner (2006) classifies piezoelectric motors into two classifications: quasistatic, and ultrasonic motors. Quasistatic motors are further characterized by those that operate on a clamping principle or inertial principle. DSM's SRM actuators are quasistatic clamping motors. A typical clamping motor operation is described in Figure 2, which follows from the Inchworm® Motor patented by Burleigh Instruments, Inc. in 1975 (May, 1975). The motor has two sets of piezoelectrically actuated mechanical clampers that alternatively grip (by applied friction) either end of the output shaft. The extender moves the clamps relative to each other and the external frame to advance the shaft either to the right or left as the sequence dictates. Through the process of clamping and unclamping the clamp elements and stepping the extender, the shaft advances.

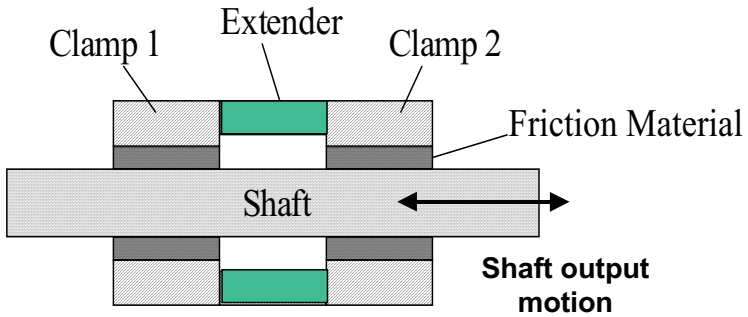

Operating sequence
1) actuate clamp 1
2) release clamp 2
3) extend shaft
4) actuate clamp 2
5) release clamp 1
6) contract mid section
7) repeat

Velocity control
step size - voltage
# of steps - frequency

Figure 2 – Operating Steps Of A Step And Repeat Motor After The Patent By May (1975)

Numerous piezoelectric motors have been developed in the last 6 years through a DARPA initiative called the Compact Hybrid Actuator Program or CHAP. Three motors demonstrated reasonably high levels of mechanical output power when compared to previous generations. Of the three motor actuators, the Kinetic Ceramic (2004) unit is the most powerful - achieving up to 40Watts of mechanical power. An advanced Burleigh unit (Burleigh, 2005) has approximately 600 times more power than the current Inchworm® motor but it produces only 2.5 Watts of mechanical power. In the UCLA MADD device (Carman et al, 2001), silicon microteeth are used but are limited in strength resulting in a 1.1-Watt maximum output. The Kinetic Ceramic motor delivers approximately 40 Watts of mechanical power through a hydraulic interface that requires hydraulic tubing and valving to deliver motion to the load.

Description of DSM's High-Force SRM Mechanism

DSM's SRM design uses a spring-biased clamper plate mechanism and other proprietary innovations within the motor to significantly improve drive force relative to current commercial SRMs. Shown in Figure 3 are the components of DSM's motor architecture. The minimal components include an extender element, a single active clamp, a static clamp, friction interface components, and the novel clamper plate. While DSM's current designs can all be operated with only one active clamp, most use two active clamps to increase the motor drive force. The extender resides directly in the moving shaft and advances the clamp element relative to the non-moving frame. In this configuration, DSM's design is an inversion of the traditional step and repeat motor with the clamper elements moving with the shaft while the location of the clamper plate remains stationary. DSM has also created a motor configuration with fixed clampers that uses the novel clamper plate and has an extender with a friction interface at each end. Either configuration with the novel clamper plate design offers higher drive forces than traditional SRM mechanisms and a means for self-compensating for temperature change and clamping surface wear.

The clamper plate provides a constant clamping force to the motor actuator enabling zero power hold. The clamping plate is on a pivot and it therefore transfers the clamping force from the active clamp to the static clamp – leading to an operating condition where the clamping force is always present. DSM's architecture also provides a much more consistent and significantly higher clamping magnitude than in the traditional step and repeat motor. For example, DSM recently developed a high-force IMPULSE PiezoMotor™ with approximately 2000 N peak force (called IMPULSE 2000 for short) and 20 mm/s peak unloaded speed. Compare this to a COTS piezomotor linear actuator from EXFO (2007) with 9.8 N peak force and 1.5 mm/s peak speed. For low-force applications and a small package, DSM is developing an IMPULSE 30 (30 N of force) with 32 mm/s drive speed.

IMPULSE PiezoMotor™ mechanism details and factors that affect the force and step size are presented relative to the components shown in Figure 3. Experimental testing results are also discussed.

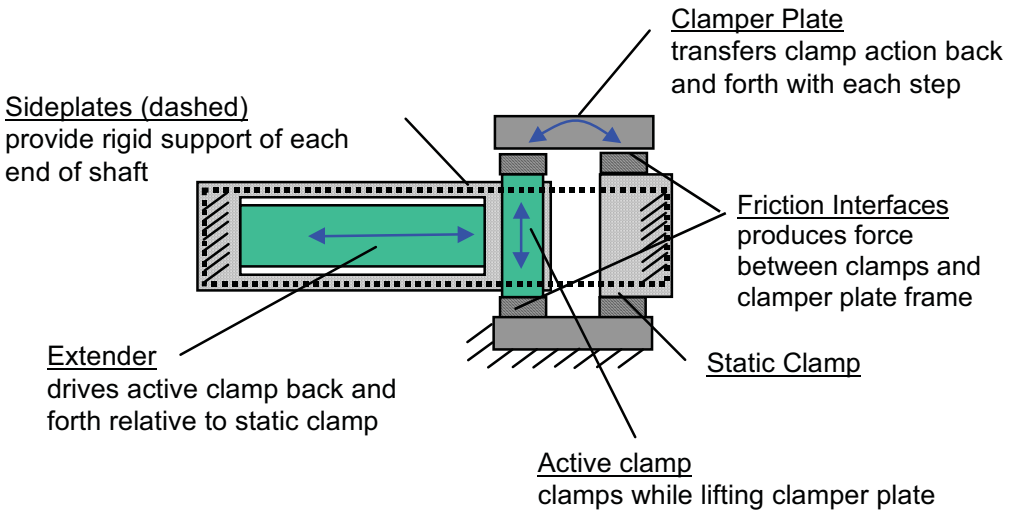

Figure 3 – Operational Components And Mechanisms In DSM's Step And Repeat Motor

Motor Drive Force

The first factor in determining motor drive force is the force capacity of the piezoelectric stack in the extender element. DSM uses two common piezoelectric stack cross-sections of 3.5 x 3.5 mm^2 and 10 x 10 mm^2. The extension force capacity of these stacks is approximately 650 and 5000 N respectively at 50 MPa of drive pressure. DSM has designed the motor's peak drive force to coincide with approximately 20% of the extender stack capacity. Therefore a design maximum for DSM's IMPULSE PiezoMotor™ with a single 3.5 x 3.5 mm^2 piezoelectric extender stack would be 130 N of drive force. To obtain up to 2000 N of drive force, DSM's IMPULSE PiezoMotor™ uses two side-by-side 10 x 10 mm^2 stacks. Figure 4 is a picture of an IMPULSE 2000 prototype motor that was delivered to a NASA valve contractor for testing with a propellant isolation valve and the IMPULSE 30 prototype.

The second factor in motor drive force is the clamping force applied by the clamper plate to the active and static clamp components. The clamping force is applied via a spring that biases the clamped plate down onto the active and static clamps. The resulting clamping force is proportional to the spring force. The product of the clamping force magnitude and coefficient of friction of interacting components dictates the driving force for the motor. The size of the spring force that can be applied to the clamper plate is dictated by the size of the piezoelectric stack used in the active clamp. A key aspect of motor design is balancing the amount of spring force with the size of the active clamp piezoelectric stack. Through careful experimentation and analysis, DSM has derived a proprietary process for sizing the spring force and piezoelectric stack for maximum driving force.

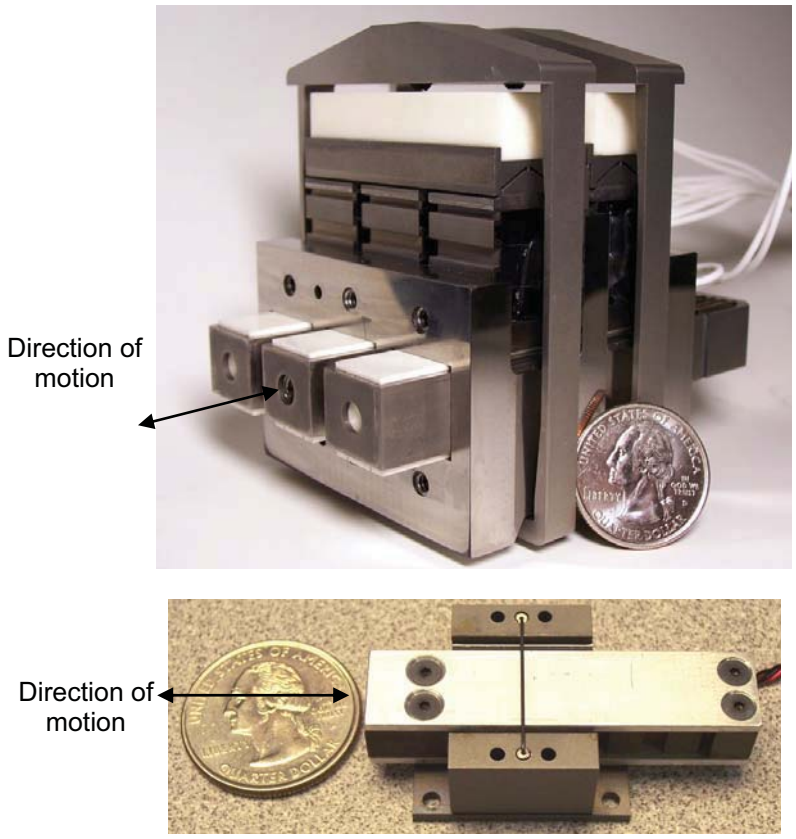

Figure 4 - Prototype Deliverable Of DSM's 2000 N IMPULSE Piezomotor™ (IMPULSE 2000) At Top And DSM's IMPULSE 30 At Bottom

A third factor in motor drive force is the friction coefficient of interfaces between the ends of the clamps and the clamper plate frame. DSM has found that the drive force is linearly proportional to the friction coefficient of the two materials in contact. Therefore, increasing the coefficient of friction between the two materials leads to an increase in drive force. DSM has performed a detailed experimental study of interface materials friction coefficients. A summary of this study is included in the next section.

Figure 5 shows the motor step size versus drive force for one of the IMPULSE 2000 prototypes and for two different IMPULSE 1000 prototypes that have been produced for NASA applications. The results were generated by driving a friction load with the motors while recording step size. Peak drive force scales approximately with the size of the clamp stacks used in the motors and with friction coefficient differences in the two systems. In this graph, the IMPULSE 2000 has more than twice the projected blocked force of the IMPULSE 1000 actuators. The IMPULSE 2000 has twice the piezoelectric clamp stack size of the IMPULSE 1000 and a coefficient of friction that is approximately 50% greater. While it is difficult to attribute specific quantitative differences to clamp size difference versus coefficient of friction, DSM has found that the trends are consistent. When a motor has twice the clamp stack size of a previous version, the available drive force can be double. When friction coefficient increases, the drive force follows.

Step Size and Drive Speed

The curve of the IMPULSE 2000 step size (Figure 5) shows a no load step of 27 microns and a near linear drop to 8-micron step size at a friction load of 2000 N. For all three prototypes, the step size consistently decreases with an increase in friction force. The difference in the step size of the two

IMPULSE 1000 motors reflects the variability in the friction between these early prototypes and the importance of achieving consistent fit and finish in the motors at the micron tolerance level.

Generally, the motor step size is dictated by the length of the piezoelectric stack used in the extender and the external load applied to the extender. Since the piezoelectric stacks are effectively spring elements, when the extender stack expands against a load, the compressive reaction force effectively reduces the stack's step size. The nature of the load also affects step size. A weight directly applied to the end of the extender will cause the extender to compress and slip backward during clamper transitions when moving against the weight. A friction load will stay in place and simply diminish the extender stroke as a function of the friction magnitude. A spring-type load will compress the extender to reach force equilibrium during each step and will release the stored energy backward during each clamper transition. In this manner, the step size becomes dependent not only on the magnitude of the external load, but also the direction and type of load.

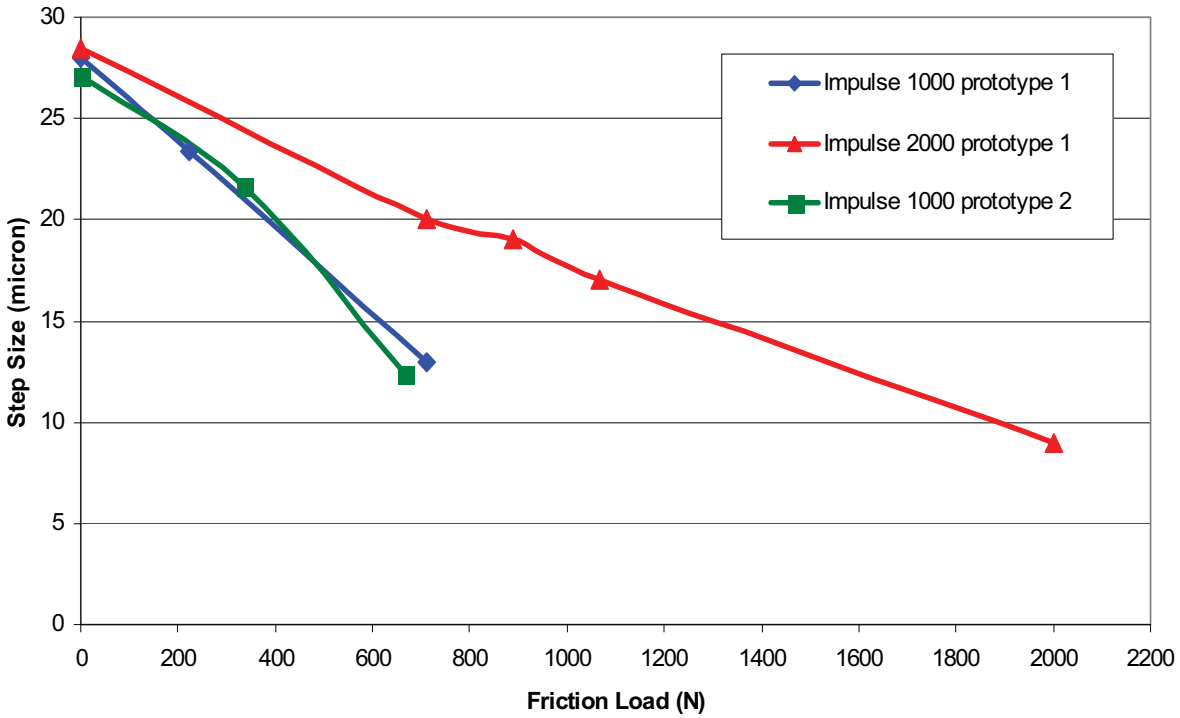

Figure 5 - Step Size Vs. Drive Force (Friction Load) For The IMPULSE 2000 And 1000 Prototypes

For example, the ideal step size and measured step size for DSM's IMPULSE 30 is shown in Figure 6. The unloaded step size of the extender using a 3.5 x 3.5 x 18 mm^3 long piezoelectric stack is 23 microns. The stiffness of this extender element is approximately 29 N/micron. Pushing a static load (weight) with this extender reduces ideal step size by the slope of the curve (i.e. 29 N static load reduces the stroke by 1 micron). This ideal step size ignores the compliance of other frame components and the non-ideal nature of the friction force that permits the motor to function. The compliance of the motor frame is a linear value that can be placed in series with the extender compliance. The non-linear friction effects are more difficult to predict but follow a recognizable trend. At this point in the SRM development, DSM has structural techniques that can be applied to reduce the motor frame compliance but has not completed a predictive model. Instead, each motor is designed with a balance of mass and stiffness to achieve the application objective while recognizing that the force versus step size response may be far from ideal.

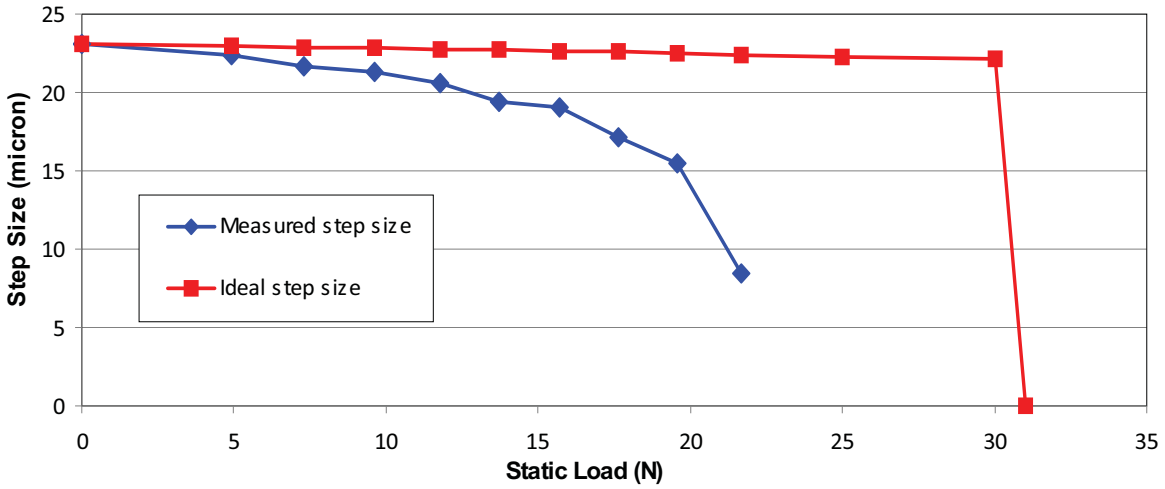

Figure 6 - Step Size Vs. Drive Force (Static Load) For The IMPULSE 30 Prototype

Drive speed is the product of the motor step frequency (number of steps per second) and the extender step size. The motor step frequency is the rate at which the electronics driver sequences the piezoelectric extender and clamper elements through the entire motor step cycle. Typical quasistatic clamping motors require that all three piezoelectric elements (extender and two clamps) oscillate through a complete square or triangle wave period without overlap in the rise or fall segments. DSM uses a special motor electronics driver that can produce six rise and fall segments fast enough to drive a 6-segment full step in less than 125 microseconds or step rate of 8000 Hz.

In practice, DSM has been able to operate motors up to 80 mm/s. The limitation results from the natural frequency of internal motor components (clamps and extender elements) being too low to respond to the highest possible step frequency. DSM can run the IMPULSE 30 and IMPULSE 2000 at approximately 2600 and 2000 steps per second respectively. The limitation in the IMPULSE 30 is the natural frequency of the extender element moving the lumped mass of the extender frame and active clamp elements. The limitation of the IMPULSE 2000 stems from the limitation in maximum piezoelectric stack preload that currently can be applied to the extender piezoelectric elements.

The fact that the piezoelectric actuator is controlled by a sequence of driving waveforms means that the motion profile can be optimized for different step frequencies within portions of the overall motion profile. This characteristic is valuable for proportional control applications.

Characteristic Impulse Force Profile

An interesting aspect of the IMPULSE PiezoMotor™ technology is the profile of the force that results during the step action. The extension step of the IMPULSE PiezoMotor™ may produce significant impact force on undamped loads. To quantify this effect, DSM tested three coupling conditions at a drive step rate of 800 motor steps per second (800 Hz). The resulting force profile measured by a high-stiffness load cell in-line with the motor extender and ground is shown in Figure 7.

At the point in the extender waveform where the extender advances the load cell into a solid aluminum block a very sharp resonance peak of 2000 N peak to peak occurs. The RMS average force is approximately 2200 N. This demonstrates the rapid hammering effect that the piezoelectric prime mover can produce against very stiff elastic loads. Placing layers of rubber between the extender and the aluminum block softens the hammering effect as shown by the blue and red curves. The impulse peaks for the 1/8th inch rubber (blue) are 1100 N peak to peak and approximately 1750 N RMS average. The impulse peaks for the 1/4th inch rubber (red curve) are 600 N peak-to-peak and approximately 1400 N RMS average.

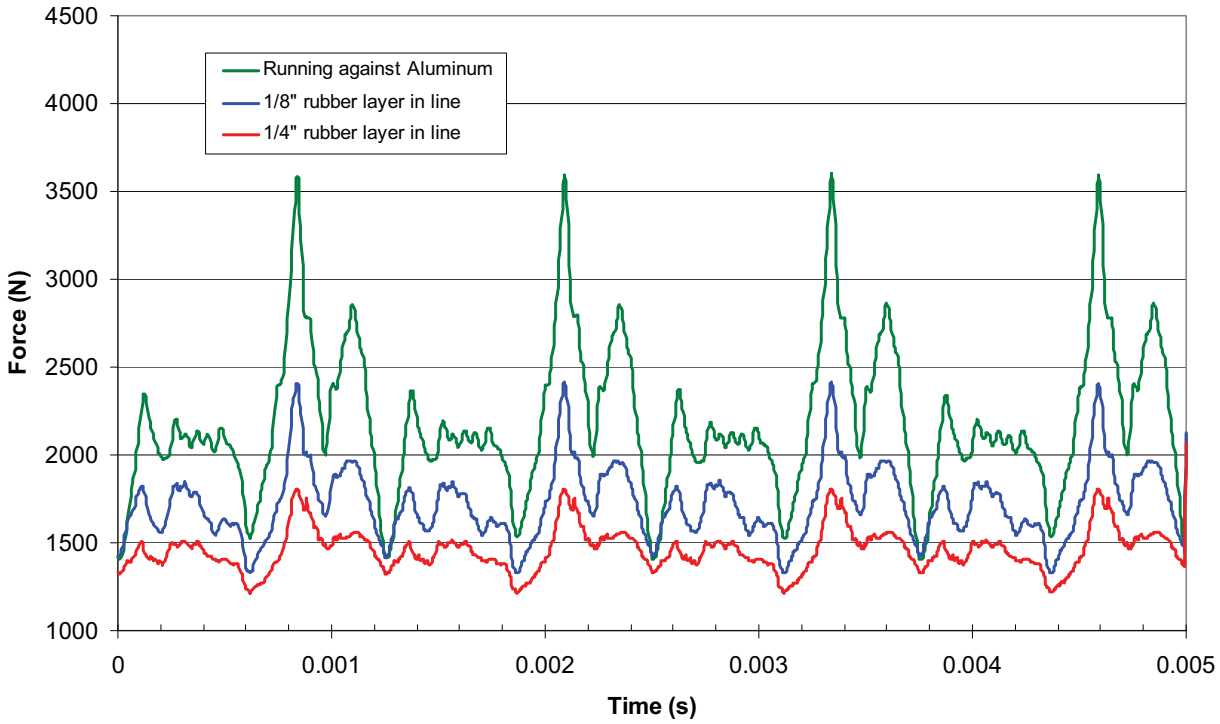

Figure 7 – IMPULSE 2000 Peak Output Force Profile With Three Different Coupling Configurations To Ground As Measured By An "In-Line" Load Cell

It is interesting to note that twice the thickness of the rubber (red curve) appears to reduce the impulse peaks to ½ the value of the blue curve. The drop in impulse peak-to-peak values appears to follow the thickness of the rubber layers. In this experiment, black neoprene rubber was used for the damping barrier but other damping and spring materials have been tested with similar results.

Characterizing the Friction Interface Materials

Because the IMPULSE PiezoMotor™ architecture is a friction-based drive mechanism, DSM has performed extensive experimental work with various material sets to understand the static and dynamic friction response. DSM has also investigated how wear affects surface roughness properties for the friction interface materials. For the IMPULSE PiezoMotor™ technology to operate properly, the friction interface materials must be very flat and smooth or have a very low surface roughness. Since the active clamp elements have stroke levels on the order of 10 to 20 microns, surface roughness values that are greater than 1 micron (40 microinch) can be significant. Additionally, the design goal is to achieve high friction at the interface materials in order to produce a high level of motor drive force. DSM has also determined that to maintain a rated load capacity, the surface roughness, flatness and parallelism of the friction pair must be maintained to an acceptable level throughout the useful life of the actuator. Therefore, minimizing wear is also a design goal.

Working with University of South Florida (Mudhivarthi, 2006) and Brigham Young University, DSM has performed a number of friction materials characterization studies for piezomotor applications. The testing consists of a series of physical tests on numerous friction pairs that was designed to simulate the loads, motions and conditions typical to the various motor applications. DSM has tested friction pairs including various combinations of steels, ceramics and surface treated steels. High-cycle wear tests were performed and optimum friction pairs for this application were identified based on high friction, low wear and low roughness. Much of this data is repeated from the work that DSM funded at University of South Florida (USF) that is recorded in the Mudhivarthi (2006) paper.

Test Method for High Cycle Friction Testing

Typical loads and speeds used in the testing were set to force and speed levels that corresponds to the drag that the friction materials would experience during a sliding transition. During a clamp move, the friction materials experience force levels up to 6000 N but with the expectation that no sliding will occur. To characterize the materials' initial hardness and surface roughness, both values were measured before any wear testing and recorded for all specimens. DSM requested eighteen material pairs to be tested by USF listed in Tables 1A and 1B.

The interaction of the friction pairs in a piezoelectric motor was simulated using a Universal Micro-Tribometer with custom fixtures. The lower test specimen (50x12x1.2 mm^3) and fixture were fixed. The upper test specimen (25x12x1.2 mm^3) and fixture provided normal loading and reciprocating sliding motion using the upper vertical and lateral positioning systems of the tribometer.

Each pair was subjected to the following test procedure:

1. Clean test surfaces with acetone before each test
2. Photograph test specimens and measure surface roughness of test specimens
3. Measure initial friction force with sliding velocity of 0.5mm/s and sliding displacement of 2mm for 3 steps with 1 sec rests in between steps
4. Perform a test sequence on the tribometer for N cycles where N is 100, 500, 10,000, 50,000, 100,000, 200,000, or 300,000, until the test is stopped due to failure or poor friction response.
    a) Set upper specimen near center of contact area of lower specimen
    b) Set normal contact force to 44.5 N (10 lb)
    c) Move upper specimen to the left 5 mm at sliding velocity of 7.5 mm/s
    d) Move upper specimen to the right 5 mm at 7.5 mm/s
    e) Repeat steps c thru d for N-1 times
5. Photograph test specimens, measure surface roughness and assess wear of test specimens

Test Results for High Cycle Friction Testing

An example of a typical friction coefficient versus time plot for a solid Croblox® sample against a 52100 steel sample is shown in Figure 8. Contrary to conventional thought, each plot in Figure 8 indicates that the initial breakaway friction (static) is less than the moving friction (dynamic). DSM attributes this characteristic to the very smooth nature of the interfacing surfaces and their lack of mechanical interaction.

Tables 1A and 1B show the test results for the coated friction interface materials and solid friction interface materials respectively. The tungsten carbide (WC) coated specimens against either a Croblox® gage block or a ceramic gage block showed very low friction. The Croblox® is a chromium carbide material from Starrett Gage Company. The diamond like carbon (DLC) coating also indicated very low friction against the ceramic gage block. These tests were therefore cancelled after only a few cycles. The response of the other coated material friction pairs in Table 1A indicate that within 40,000 cycles, the coating had abraded enough that is was decided to stop the test. The coatings were generally 2 to 5 microns (80 to 200 microinch) thick. Therefore, surface roughness on the order of 2 microns (80 microinch) is an indication that the coating thickness might be completely worn away. Generally, after abrasion on the surfaces exceeded 2 microns (80 microinch) the test was stopped. The trends indicate that the surfaces with higher initial coefficient of friction (COF) had greater abrasion after fewer cycles.

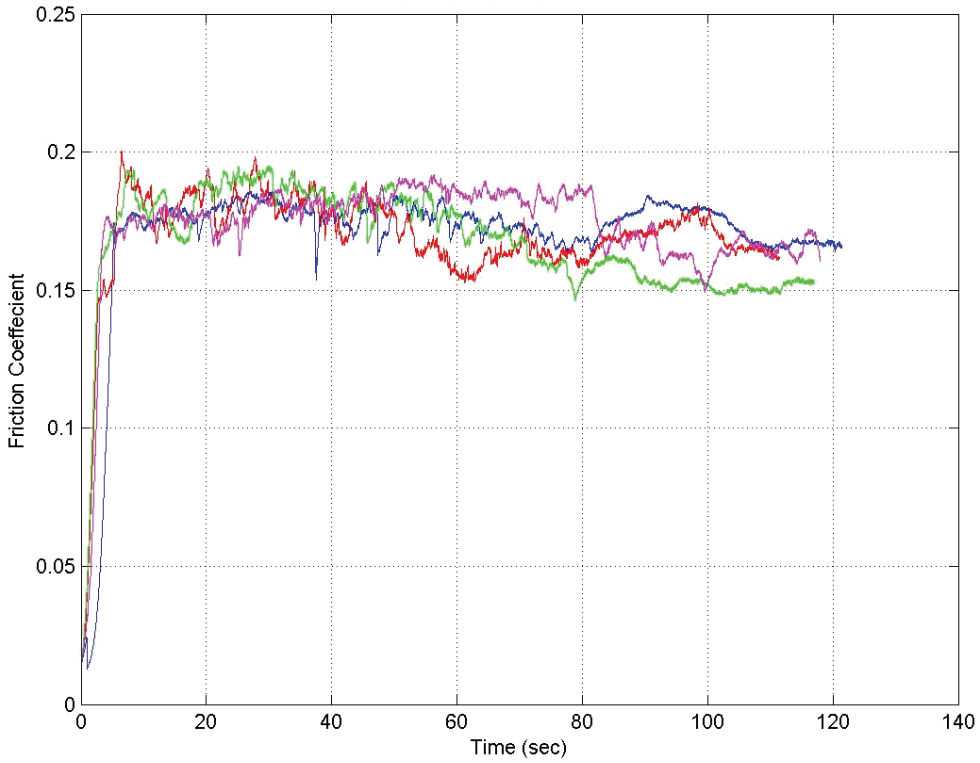

Figure 8 - Friction Versus Time Plot For A Solid Croblox® Against A Solid 52100 Steel Specimen

Table 1A - High Cycle Tests Summary For Coated 52100 Steel Friction Interfaces
(repeated from Mudhivarthi, 2006)

No.	Material Pair	COF	Post Test Condition
1	TiN / TiN	0.18-0.22	Coating removal/severe abrasion after 600 cycles; Rtm=41-364 μin
2	MoST / MoST	0.10-0.32	Severe coating removal after 100 cycles; Rtm=45-177 μin
3	WC / ceramic gage block	0.09	Cancelled due to low friction
4	WC / 52100 steel gage block	0.18-0.21	Abrasion after 20,000 cycles; Rtm=33-65 μin
5	WC / Croblox® gage block	0.11	Cancelled due to low friction
6	DLC / ceramic gage block	0.09-0.11	Cancelled due to low friction
7	DLC / 52100 steel gage block	0.13-0.15	Abrasion after 40,000 cycles; Rtm=14-96 μin
8	Tetrabond / ceramic gage block	0.17-0.21	Abrasion after 20,000 cycles; Rtm=79-94 μin
9	Tetrabond / 52100 steel gage block	0.32-0.36	Severe abrasion after 10,000 cycles; Rtm=79-156 μin
10	TiN / A2 steel	0.16-0.24	Severe abrasion after 10,000 cycles; Rtm=280-1,257 μin

The solid material friction interface pairs (Table 1B) performed very well in terms of wear and surface roughness. The steel feeler gages cycled against each other were the only pair that manifested severe abrasion after a relatively low number of cycles. Compared to the coated specimens, the solid friction interface materials had much lower abrasion and lasted to levels of 300,000 cycles in the case of ceramic on ceramic. When comparing the response of the materials, DSM found that the following pairs had reasonable coefficient of friction levels in the range of 0.12 to 0.18 and indicated very mild abrasion:

- Sapphire on 52100 steel gage block (test no. 14) at 0.13 to 0.15 COF,
- Sapphire on ceramic gage block (test no. 15) at 0.15 to 0.17 COF,
- 52100 steel gage block on ceramic gage block (test nos. 12 and 17) at 0.12 to 0.17 COF, and
- Ceramic gage block on ceramic gage block (test no. 18) at 0.13 to 0.15 COF.

For environments where resistance to corrosion is an issue, the two different ceramic pairs would perform better than either of the two pairs with steel. Fine particles generated during testing of the 52100 steel gage block on ceramic gage block were found to be oxidized and some of the fine abrasive scratches in the steel also showed oxidation.

Table 1B - High Cycle Tests Summary For Solid Material Friction Interfaces
(repeated from Mudhivarthi, 2006 with updates*)

No.	Material Pair	COF	Post Test Condition
11	Steel feeler gage / steel feeler gage	0.30-0.60	Severe abrasion after 600 cycles; Rtm= 1.4 – 3.1 μm (57-123 μin)
12	52100 gage block / ceramic gage block	0.14-0.17	Mild abrasion after 200,000 cycles; Rtm= 0.1 – 1.2 μm (4 - 47μin)
13	Croblox® gage block / ceramic gage block	0.13-0.2*	Cancelled due to low friction
14	Sapphire / 52100 steel gage block	0.13-0.15	Mild abrasion after 40,000 cycles; Rtm= 0.1 – 0.2 μm (5 - 10 μin)
15	Sapphire / ceramic gage block	0.15-0.17	Mild abrasion after 40,000 cycles; Rtm= 0.08 – 0.2 μm (3 - 7 μin)
16	Croblox® gage block / 52100 steel gage block	0.15-0.2*	Abrasion after 10,000 cycles; Rtm= 0.08 – 1.1 μm (3 – 46 μin)
17	52100 steel gage block / ceramic gage block	0.14-0.2	Mild abrasion after 200,000 cycles; Rtm= 0.08 – 1.4 μm (3 – 55 μin)
18	Ceramic gage block / ceramic gage block	0.13-0.15	Mild abrasion after 300,000 cycles; Rtm= 0.08 – 0.1 μm (3 – 5 μin)

Example of Wear at the Friction Interface

To characterize the material wear of friction surfaces within a prototype piezoelectric motor environment, DSM assembled an extender element using two 52100 steel gage blocks separated by a piezoelectric extender stack. The extender was actively driven within an early IMPULSE PiezoMotor™ prototype frame. The mating friction surfaces contacting the extender's steel gage blocks were fabricated from a hard ceramic. Following a cumulative travel distance of 10 km, surface profile scans were made on the extender's blocks in order to quantify material loss. The mating ceramic surfaces were not profiled. The surface scans were performed along the direction of the lines indicated in light blue in Figure 9.

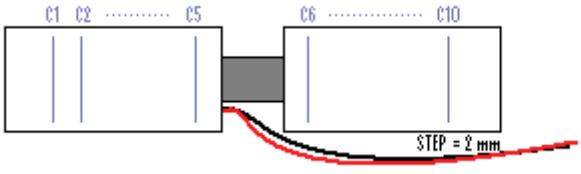

Figure 9 - Sketch Of Extender Assembly Used In Long Endurance Friction Wear Testing

Figure 10 illustrates the surface height measured with a profilometer for each of ten scans. Note the original flatness of the block on the outside edges. Over the course of ten kilometers, as much as ~8 microns of depth in the steel was worn away in certain locations, but the average material loss appears closer to 4-5 microns of depth. One attractive feature of DSM's IMPULSE PiezoMotor™ patent-pending

architecture is its ability to compensate for this material loss, thus avoiding a decrease in the motor's available driving force.

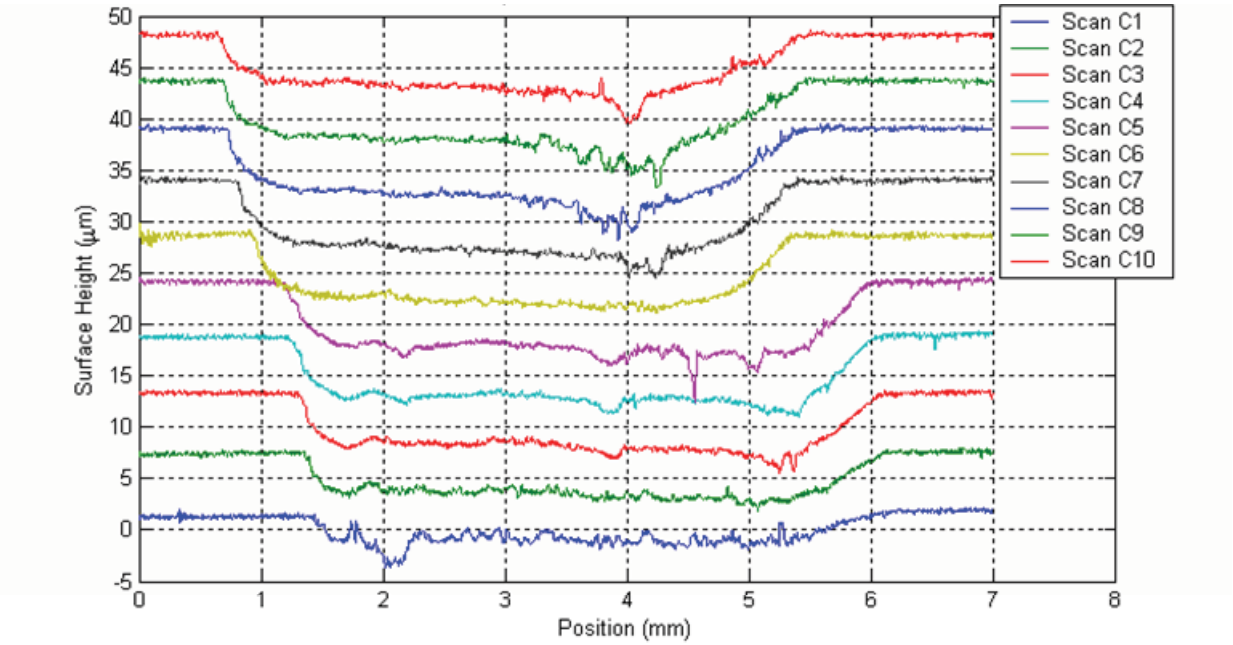

Figure 10 - Surface Heights For Each Of Ten Scans Across The 52100 Steel Extender Components After 10 km Of Cumulative Linear Travel In A Prototype Piezoelectric Motor

Conclusions from the Study of Friction Interface Materials

A number of coated and solid friction interface materials have been studied and tested. The solid friction materials held up substantially better than the coated friction materials. Three types of materials held up notably well: a ceramic gage block; a hardened 52100 bearing steel; and, a sapphire substrate. All indicated very little abrasive wear in a friction test at over 40,000 wear cycles. Of particular interest is the nature of the coefficient of friction in the hardened specimens. Regardless of the initial COF, all of the materials migrated to a similar range of 0.11 to 0.18 COF after sufficient wear cycles had occurred.

Accuracy and Resolution of the SRM Mechanism

As described previously, the step size of DSM's SRM mechanism is dependent on the size of the load applied to the motor output. The accuracy of the step size is therefore dependent on the load magnitude and the consistency of the load. Generally, DSM recommends that these mechanisms be used with an encoder or other type of position feedback device to provide a means of updating the position to the controller and closing the position loop on a specific target.

In a recent example of using an IMPULSE 1000 to drive a NASA valve, DSM closed the loop on a position target using an LVDT device for feedback. An LVDT produces a linear variable voltage as a function of position over the travel length. In this application, the SRM was used to drive the valve to a set location (voltage). The controller is programmed to stop the motor at the nearest step position within a designated deadband around the voltage position target. In this case, the resolution of the position control is approximately one motor step or less than 25 microns.

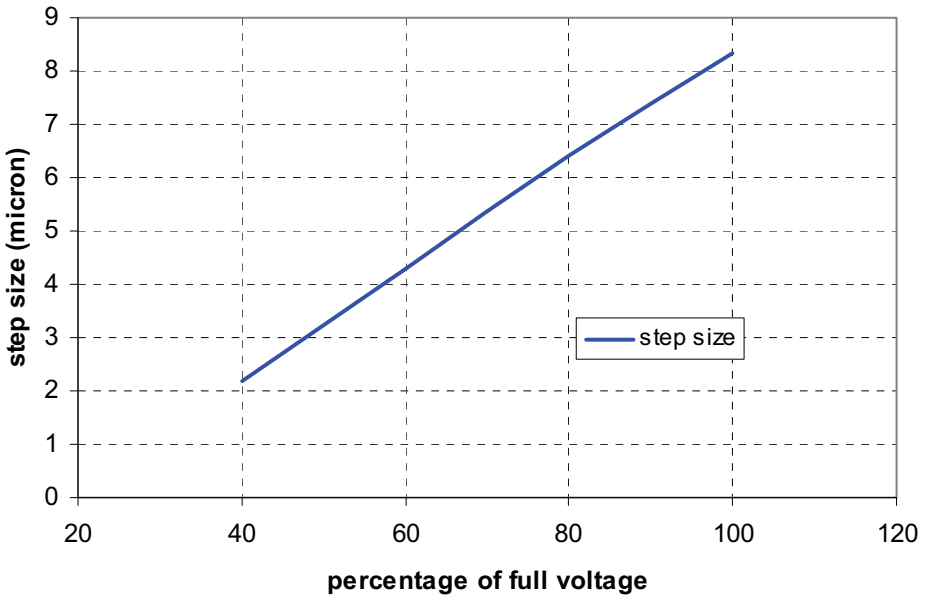

Figure 11 – Demonstration Of Partial Stepping On An Early SRM Prototype

In another demonstration to test the capability for producing micro-stepping in an IMPULSE PiezoMotor™ device, DSM ran an early "light duty" SRM with a variable voltage on the extender. Figure 11 shows the resulting step size as this motor was driven a few steps to characterize the step size. The partial step size follows the voltage applied to the extender in a linear and proportional manner indicating that overall resolution of the motor might be made smaller using proportionally smaller extender steps.

Measurements of Electrical Power Input to the IMPULSE PiezoMotor™

Using an accurate data acquisition setup, DSM engineers measured the electrical power going into each channel of the IMPULSE 30 prototype as a function of drive voltage, step rate and static load (weight) applied to the output of the motor. Two different drive voltages, multiple drive step frequencies and multiple static load values were tested. The outcome of the testing is captured in Figure 11. DSM used linear amplifier electronics in this study to make the measurements; current and voltage signals are better captured with linear amplifiers instead of motor electronics. With the linear amplifiers, the step rate was limited to 500 steps per second.

To make a measurement of output power efficiency, DSM measured the output mechanical power of the motor while pulling a range of static loads (weights). DSM found that the efficiency was very low since the extender stack has much more mechanical force capacity than can be manifested by the clamping elements. In other words, the main pushing stack of the motor can produce 130 N (30 lbf) of drive force but is only called upon to produce up to 30 N (7 lbf) of drive force because of clamp limitations. Since DSM's motors are friction limited, the excess capacity of the extender simply goes to waste.

Figure 12 shows the electrical power used to drive the motor as a function of static load (weight) that the motor is lifting. The electrical power measurements were made for each channel (extender and clampers) along with the motor displacement for 25 steps at 200 steps per second while lifting the indicated mass. The mechanical power is the product of lifting force and motor velocity. At 200 Hz, the velocity is approximately 4.5 mm/s under zero weight. Velocity decreases with increased lifting mass as indicated by the green displacement line. The peak mechanical power correlates with lifting around 1800 grams (3.5 lbm).

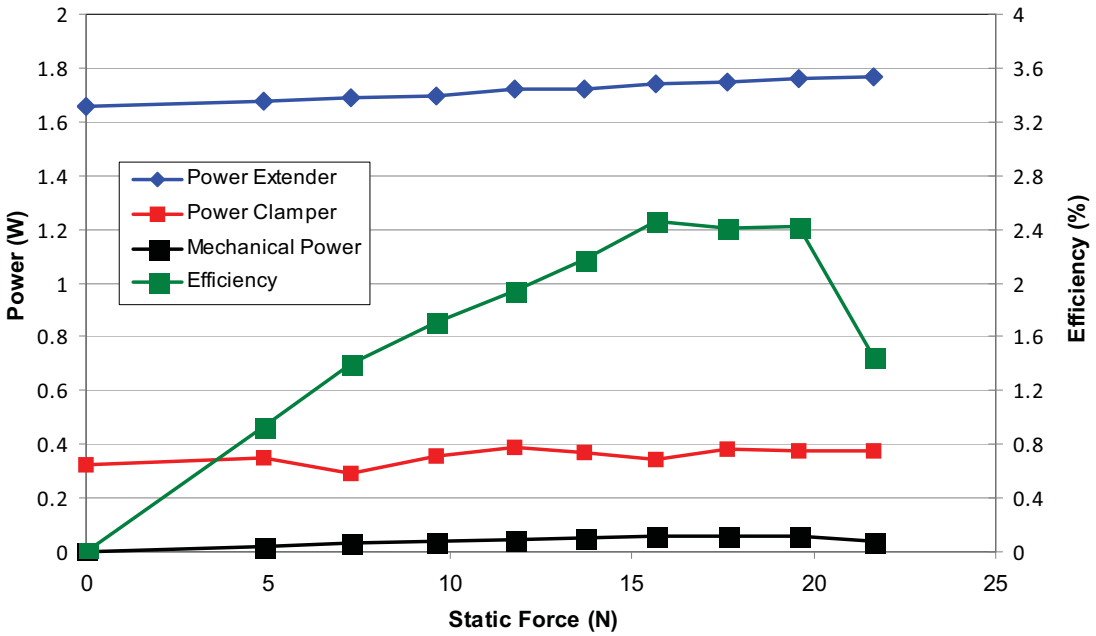

Figure 12 – Electrical Power Used In DSM's IMPULSE 30 At 200 Hz Step Rate

From this data, DSM gains information regarding how the electrical power is used in the motor actuator. First, the clamp stack electrical power does not vary as a function of the mass that the motor is lifting. The extender channel electrical power shows only a small correlation with the increased mass and even with no lifting mass, the extender uses over 1.6 Watts of power. The small increase in extender power correlates with the increase in mechanical power indicating that any work that the extender is required to produce while lifting mass requires proportionally more electrical power.

The mechanical power increases with the lifting force until the motor drive force becomes friction limited. Once the lifting force exceeds the available friction force, the motor begins to slip during its forward motion and the mechanical power decreases. The efficiency is the measure of the output mechanical power divided by the total electrical power applied to the motor. Peak efficiency numbers are approximately 2.5%. DSM estimates that there are two reasons for the low efficiency numbers. The first involves the oversized nature of the extender stack used in the motor. The second reason involves the electrical properties of the particular piezoceramic material that this motor uses.

Using a smaller extender stack can cause the motor efficiency to increase since the motor drive force is friction limited not limited by the extender stack size. Another method for increasing the efficiency of the motor would be to use piezoelectric ceramic materials that are by composition more efficient than the soft PZT materials used in the current motor prototype. The current motor prototype uses piezoelectric ceramics with a loss factor of over 5% and a relatively high amount of capacitance. DSM is considering the use of piezoceramics with less than 40% of the loss factor and approximately 50% of the capacitance of the soft piezoelectric ceramics. DSM estimates that this might lead to a doubling of the current efficiency numbers.

Piezoceramic motors have a significant advantage in duty cycle over electromagnetic motors. In actuator duty cycles where holding maneuvers are required, DSM's motors use only the quiescent power that is required to maintain the drive electronics in a ready state. The piezoelectric motors do not require any power to hold position. Therefore, even 18 Watts of power for the 10 to 20 ms used to make a move does not require significant battery energy. With the same setup, DSM measured the power as a function of step rate for the IMPULSE 30 SRM. The power was measured for step rates up to 500 steps per second and then extrapolated for higher frequencies. DSM found a direct linear correlation between electrical power going into the motor and step rate.

Conclusions

In the IMPULSE PiezoMotor™ technology, DSM has developed a new class of high force piezoelectric SRM mechanisms. The operation of the motor and the drive force, step-size, and characteristic step impulse profile are presented. Compared to conventional step and repeat motors, DSM has produced a family of devices with substantially greater drive force. Results from a study of various potential friction interface materials yields a set of materials with suitable wear performance and with coefficients of friction that are in the range of 0.15 to 0.18. Modulating the voltage on the SRM extender to obtain smaller steps is demonstrated as a means to increase the step resolution of the output. To demonstrate the electrical to mechanical conversion potential in the SRM mechanisms, DSM performed an experimental study that involved lifting various weights and measuring resultant speed. For the current family of actuators, drive efficiency is around 2.5%. A means of obtaining higher levels of drive efficiency is discussed. Measurements also indicate that the electrical power increases proportionally to the motor step rate.

The proposed actuators offer the following significant advantages over conventional electromagnetic actuator technologies.

- the ability to withstand higher (200°C) and lower (-150°C) temperatures,
- zero power draw during hold maneuvers,
- the ability to carry a significant side load,
- greater impact resistance due to the solid-state nature of their construction,
- fewer number of components that leads to a more reliable system,
- lack of required lubricants for improved storage characteristics, and,
- a much smaller form factor for the same level of force.

References

Spanner, Karl, 2006, “Survey of Various Operating Principles of Ultrasonic Piezomotors, Proceedings of Actuator 2006, June 9, 2008, Bremen, Germany.

Carman, Dunn, Friedmann, Hahn, Ho, Kim 2001, “Developing Innovative Actuator Devices for Use on Rotocraft Systems” U.S. Army Research Office.

Burleigh, 2005, “Prototype Actuators”, The Power of Precision, Burleigh, An EXFO Company.

Kinetic Ceramics, 2004, “High Pressure Piezoelectric Pump”, Kinetic Ceramics website: http://www.kineticceramics.com/pdf_files/turnkey_pzt_systems.PDF

EXFO, 2007, Inchworm Motors W-800/810, Web page specification sheet at http://www.exfo-lifesciences.com/nano/app_notes/IW-800.pdf

May, William, 1975, “Piezoelectric Electromechanical Translation Apparatus, U.S. Patent 3902084, Aug. 26, 1975.

Mudhivarthi, S., D. P. Hess, 2006, “Wear data from friction pairs for microscale piezoelectric actuators”, in Tribotest, Volume 11, Issue 1 , Pages 1 – 10, Published online 9 Mar 2006.